DAMAGE ACCUMULATION IN GRAPHITE-EPOXY COMPOSITES DURING COMPRESSIVE FATIGUE

Chris Byrne, Joseph W. Krynicki and
Robert E. Green Jr.
Center for Nondestructive Evaluation
The Johns Hopkins University
Baltimore, MD 21218

INTRODUCTION

There has recently been considerable interest in the behavior of thick section (one inch and greater) polymer composites under compressive loads [1]. Strength, fatigue life and damage modes are characteristics which design and inspection engineers seek to understand to properly utilize these materials in applications where compressive loads are encountered. This paper presents a brief summary of some of the progress in a research effort to characterize the compression-compression fatigue behavior of thick section fiber reinforced polymer composites. Primary objectives of this research are to determine fatigue life and strength, and to use nondestructive techniques to predict material failure with particular interest in identifying the early stages of damage. Destructive techniques are implemented to correlate actual damage mechanisms to any "fingerprint" found by NDE methods. Specifically, one inch thick, double edge notched, graphite epoxy coupons were fatigued to failure while structural stiffness and acoustic emissions were monitored. Unfailed specimens were examined using ultrasonic C-scan and X-ray radiography after which they were cut and polished for damage identification via microscopy.

Most of the work on fatigue of composites that is found in the literature has been from tension-tension or tension-compression fatigue of relatively thin composite laminates [2,3]. Though much has yet to be learned in this area, there does exist a certain "state of the art" knowledge regarding composites under fatigue. In particular, specific damage modes are known to occur in a certain sequence as damage develops in a composite laminate. Failure of the fiber-matrix interface occurs first as transverse matrix cracks (TMC) in off load axis plies. These TMCs occur with a periodic spacing which is a function of the constituent material properties and ply lay-up. Eventually the plies become saturated with these cracks, a condition referred to as the characteristic damage state. Secondary cracks develop in plies aligned with the load axis (longitudinal matrix cracks - LMC) due to several potential sources. In one case there is sufficient stress concentration built up where a TMC meets the ply interface to initiate a LMC. In another scenario shear stress in the fiber direction causes this LMC. When a TMC induces a LMC there exists a stress concentration at their intersection ideal for the initiation of a delamination. Next cracks begin to couple, delaminations form and grow. All along fiber breaks occur but now they fail on a localized scale. At this point the composite is at the end of its expected life and total fracture is imminent.

Review of Progress in Quantitative Nondestructive Evaluation, Vol. 12
Edited by D.O. Thompson and D.E. Chimenti, Plenum Press, New York, 1993

Mechanical characteristics have been used to monitor the condition of composites subjected to fatigue. Correlations have been made between structural stiffness degradation and specific types of damage in the material. For instance, a drop in stiffness during the first 20% of life has been found to parallel the accumulation of TMCs right up to reaching the characteristic damage state where stiffness change tends to level off [4]. Another relatively large reduction in stiffness occurs near the end of fatigue life. This corresponds to fiber breaks on a localized scale. The value behind understanding stiffness changes is reflected by the fact that some researchers use this characteristic to develop models which predict composite fatigue life [5].

Failure theories for composites under a compressive load exist which focus on the stability of the fibers as the determining factor controlling failure [6]. Matrix toughness and modulus play an important role in maintaining fiber stability. Aside from this, a review of recent literature found no work which looks at failure due to compression-compression fatigue and the sequence of damage which leads to fiber instability and, ultimately, fracture.

EXPERIMENTAL

The material used was a graphite-epoxy prepreg tape supplied by Hercules (AS4/3501-6). Panels measuring 12" by 12" were manufactured with a $(0_2,90)_{32,S}$ layup having a nominal thickness of one inch. Panels were cured using an autoclave process which results in fiber volume fraction of approximately 62%. Specimens cut from this panel measured three inches in height and one inch in width. One eighth inch radius stress concentration notches were cut into both sides of each specimen at their mid-height to localize fatigue damage for optimal monitoring by nondestructive methods (insitu monitoring of ultrasonic attenuation, infrared thermography and surface morphology changes by laser speckle decorrelation were some techniques used which will not be discussed in this paper). Specimens were epoxied into 1/4" recessed steel endcaps to prohibit brooming and end splitting of the composite while allowing the load to be applied through the specimen end. A 110 kip capacity MTS 810 load frame equipped with parallel platens and interfaced with a PC was used for mechanical testing and data acquisition. A one inch gauge length extensometer was mounted symmetrically about the stress concentration notch to measure axial strain. Specimens were then set in the load frame and a 200 lb compressive preload was applied. Fatigue cycles were load controlled using a 1 Hz haversine fatigue cycle to maximum loads ranging from 76% to 94% of the specimen ultimate strength. A schematic of the test specimen and equipment is shown in Figs. 1 and 2.

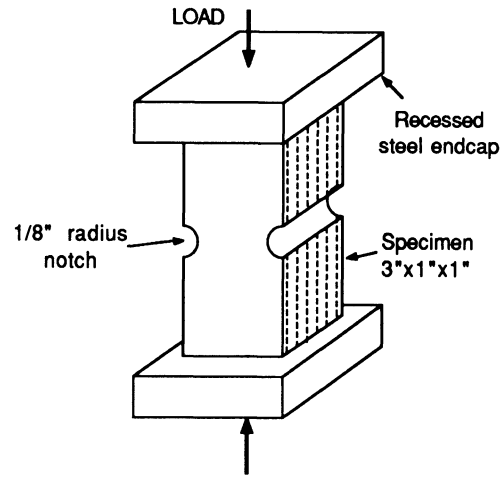

Fig. 1. Test specimen schematic.

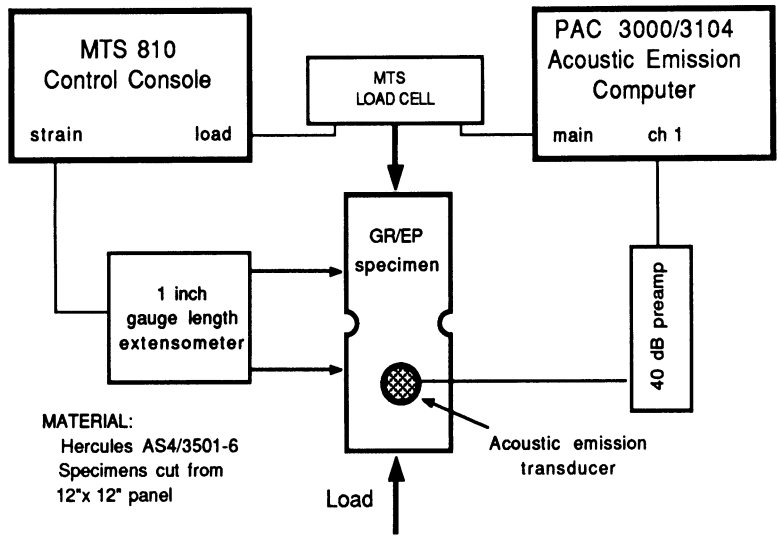

Fig. 2. Equipment schematic.

Acoustic emissions were monitored by a Physical Acoustics Corporation acoustic emission transducer having a nominal frequency of 125 kHz. Sensor preamplification was 40 dB with a signal band pass filter of 100 kHz to 300 kHz. A PAC 3000/3104 acoustic emission analyzer was used for data storage and manipulation and was set to provide a threshold of 58 dB (1 microvolt base) to omit background noise. Acoustic emissions were continuously monitored during fatigue cycling.

X-ray radiographs were obtained with a Hewlett Packard Faxitron cabinet system using Kodak ultra-speed dental film. A radio-opaque penetrant solution containing zinc iodide was used to enhance the defect regions in the composite. Photomicrographs of specimens that were cut and polished were obtained using a Leco Neophot 21 metallograph.

RESULTS AND DISCUSSION

The trend in stiffness reduction for specimen D27, cycled at 68 kip maximum (87% of ultimate strength), is shown in Fig.3. Stiffness is observed to increase after the first cycle in the fatigue test. This is attributed to a reduction of the effect of the stress concentration notch due to longitudinal matrix cracks at the root of the notch. This observation is consistent with a increase in residual strength reported by Lagace and Nolet [7]. After the second cycle stiffness decreases until approximately 20% of specimen life where it remains virtually constant. Just before failure a sharp reduction in stiffness is recorded. This trend has similarities to that observed during tension fatigue tests as reported by Stinchcomb and Bakis [4]. Correlations to specific compression-compression damage modes responsible for these trends are currently being sought. Also shown in Fig. 3 is an increase in permanent deformation with fatigue. This is the strain at the no load portion of the fatigue cycle and follows a similar trend as the stiffness except that during the first 20% of fatigue life the permanent strain changes at a faster rate.

A plot of the second cycle in a fatigue test for two different tests is shown in Fig. 4. One of the cycles is from a specimen which had no notch at its mid-length. This is compared to a cycle from a conventional, double edge notched, specimen. It can be seen that the notched specimen exhibits a hysterisis while the unnotched specimen does not. The hysterisis of the notched specimen has been observed to increase with fatigue.

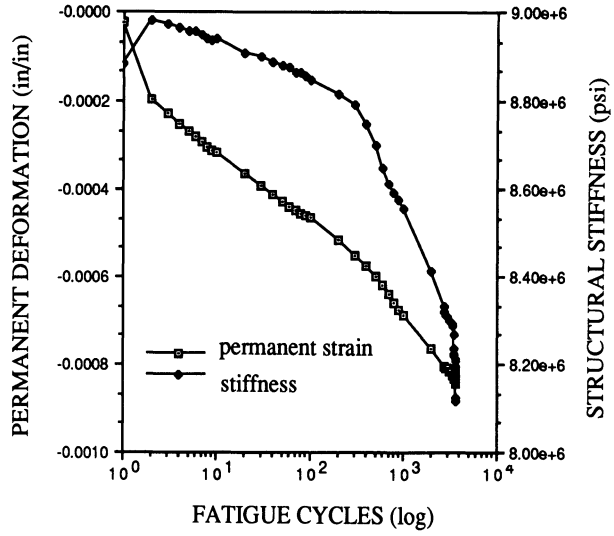

Fig. 3. Structural stiffness and permanent deformation for specimen D27.

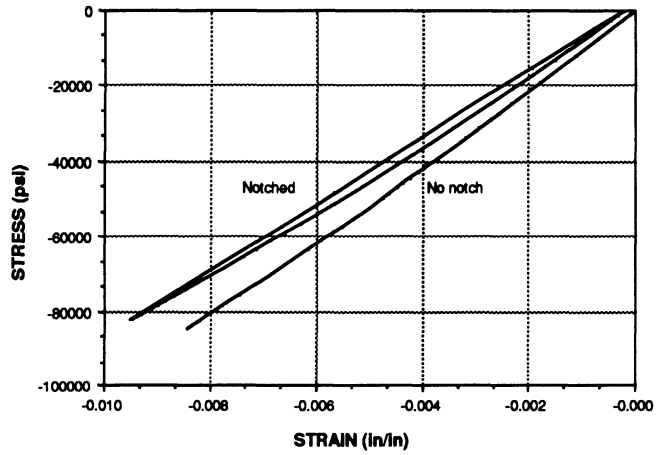

Fig. 4. Stress/strain diagram indicating the different response of a notched specimen and straight sided specimen.

Acoustic emission data from specimen D27 is shown in Fig. 5a. Note the time axis is equivalent to fatigue cycles since a 1 Hz cycle was used. The graphs show high amplitude events occur at the beginning and end of specimen life with sporadic high amplitude events throughout fatigue test. Figure 5b is from the same test but represents only the events occurring at the higher loads of the fatigue cycle (> 60 kip). Low load events have been filtered out. With virtually no difference between figures 5a and 5b we conclude that the majority of the highest amplitude events occur at the high load portion of the fatigue cycle. Acoustic events versus fatigue life for the entire load cycle and load filtered are shown in Figs. 6a and 6b. The rate at which events occur throughout the fatigue test shows no apparent trend. When load filtered however, we observe that the beginning and end of specimen life has the highest rate of events. This acoustic activity at the beginning corresponds to the rapid change in strain readings observed. Also, we note, a great many events actually occur during the low load portion of the fatigue cycle. This is contrary to intuition which tells us that acoustic emissions occur with crack propagation as a source which would normally occur at the highest loads in the cycle. Another source should therefore be responsible for these low load events. One such source could be internal rubbing surfaces.

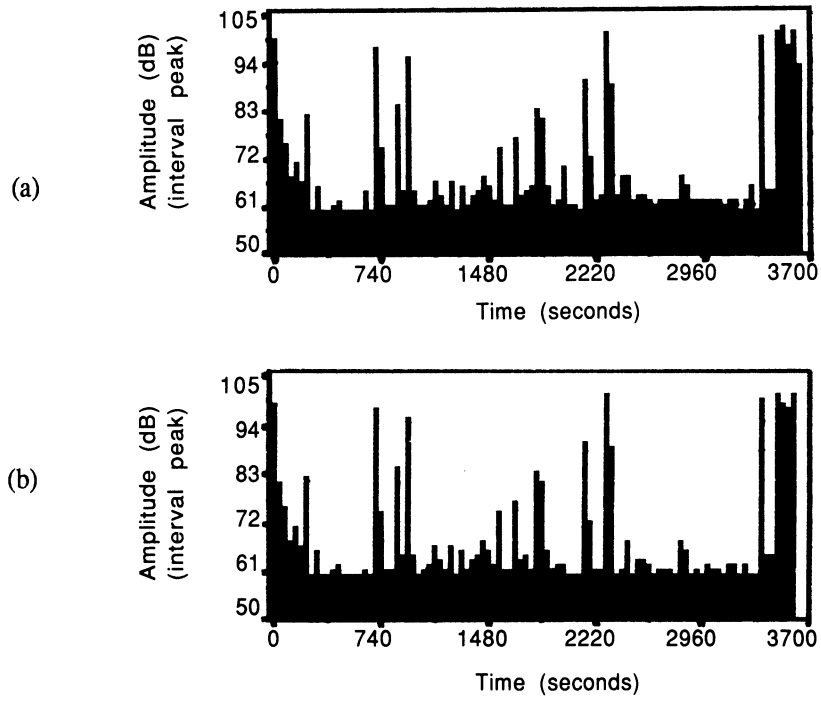

Fig. 5. Acoustic emission data from specimen D27. (a) interval peak amplitude of events for entire load cycle, and (b) interval peak amplitude which has been load filtered to exclude events during portion of cycle less than 60 kip. Note: one second equals one fatigue cycle.

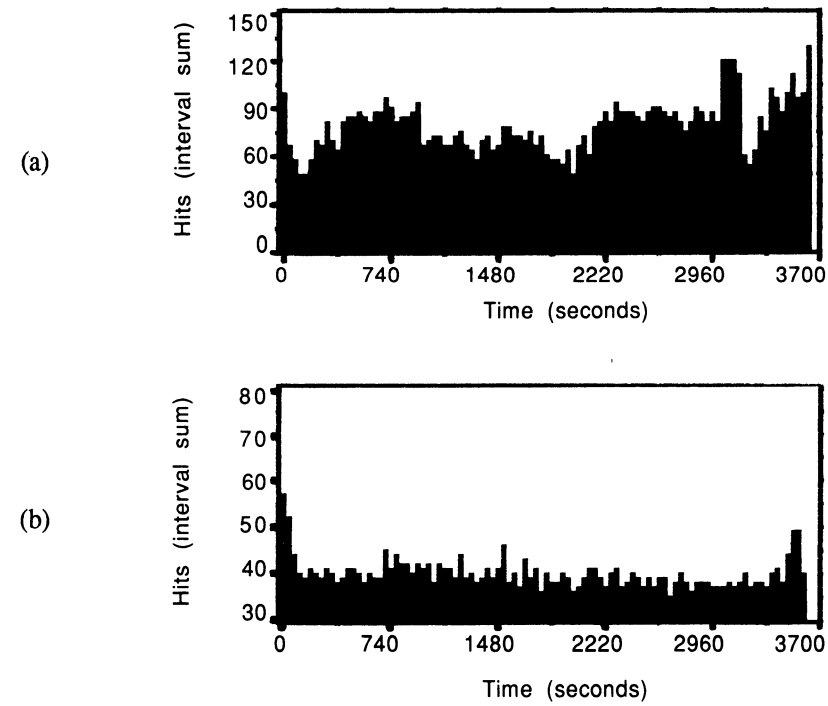

Fig. 6. Acoustic emission data from specimen D27. (a) detected events ("hits") on an interval sum basis for entire load cycle, and (b) detected events on an interval sum basis which has been load filtered to exclude events occurring during portion of cycle less than 60 kip. Note: one second equals one fatigue cycle.

An image from a penetrant enhanced x-ray, viewed through the thickness, of a specimen which had been fatigued to the end of its expected life (as determined by stress life curves generated by other specimens) is shown in Fig. 7. Damage appears as dark regions in the image and consists of two types. First, LMCs are indicated above and below the stress concentration notch as a series of dark lines. Second, cracks passing through both 0^{o} and 90^{o} plies are present at the root of the notch. These cracks result from kink band formation which leads to shear failure of the fibers in the 0^{o} plies. A third type of damage is found when x-rayed in the plane of the lamina as seen in the radiograph of Fig. 8. The region of shear failure previously noted is clearly observed. The dark lines extending above and below are edge views of ply delaminations. These same delaminations were imaged by ultrasonic C-scan performed through the thickness of the laminate.

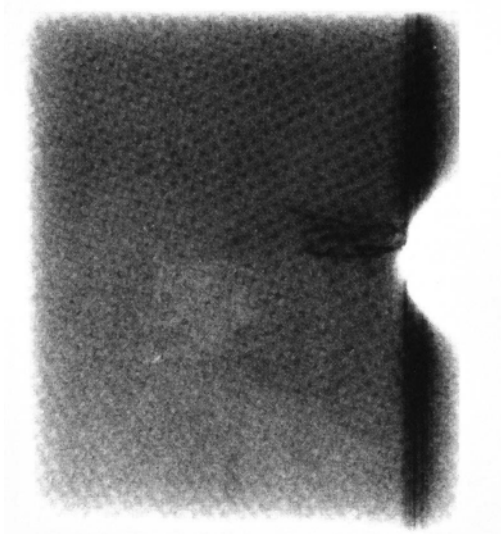

Fig. 7. Radiograph of unfailed specimen showing longitudinal matrix cracks above and below notch. Shear failure of plies with fibers aligned with the load axis is seen at base of notch.

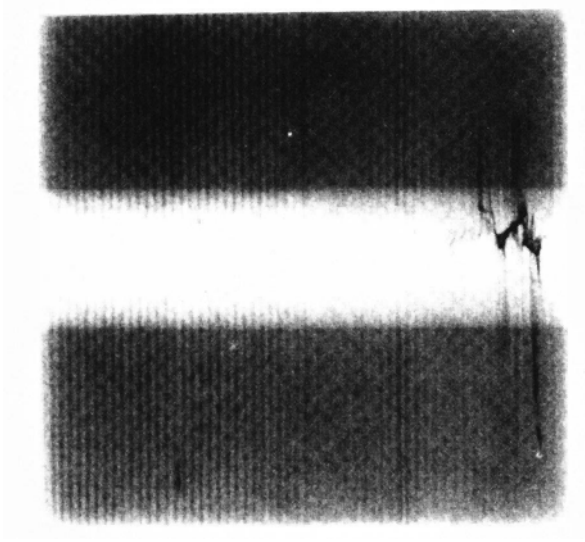

Fig. 8. Radiograph of specimen shown in Fig. 7 (viewed from the right) with notch seen as the light region in the middle. Shear failure displays a saw tooth pattern within notch. Delaminations are evident above and below saw tooth.

Destructive evaluation of fatigue damage was performed by sectioning and polishing specimens for identification via microscopy. The photomicrograph in Fig. 9 shows a LMC in one of the 0_2 plies in a specimen. Also shown is a delamination originating at the specimen free edge and terminating at the LMC. It is well established that interlaminar shear and normal stresses cause free edge delaminations which, in many cases, propagate completely through the composite during fatigue testing. However, the specimen geometry used in this research has not exhibited this tendency apparently due to the presence of LMCs (except for delaminations which occur with complete failure of specimen). A typical TMC is shown in the photomicrograph of Fig. 10. The specimen used had been fatigued past its expected life and was saturated with this damage. The crack is observed to pass through some fibers but not to the ply interface. The fact that it does not reach the lamina interface is significant yet not surprising. Since there is no extensional mode in the fatigue cycle there is virtually no driving force for the crack to propagate through the ductile matrix. Since the crack is not at the ply interface there is not going to be the same stress redistribution to initiate secondary forms of damage as found in tension fatigue tests.

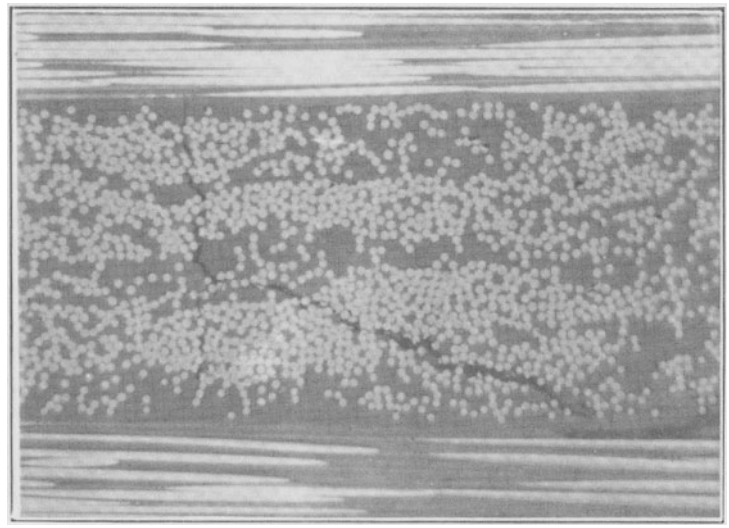

Fig. 9. Photomicrograph of fatigue damage illustrating a ply delamination arrested by a longitudinal matrix crack. Specimen free edge is to the right of the image. View is along the load axis.

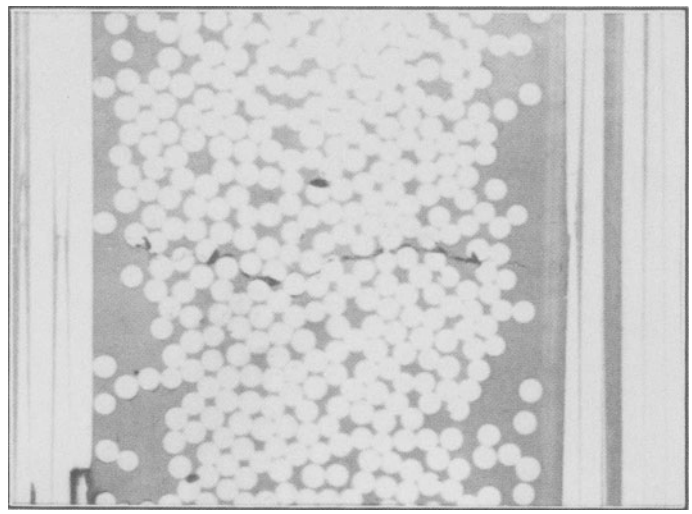

Fig. 10. Photomicrograph of a typical transverse matrix crack. Load was from the top and bottom of picture.

CONCLUSIONS

Results from mechanical testing indicate that damage does accumulate throughout fatigue as reflected by the change in structural stiffness of the specimen. Also demonstrated was increased permanent deformation with fatigue. Mechanical hysterisis was determined to result from the presence of stress concentration notches. Acoustic emission results gave higher amplitude and higher rate of acoustic events at the beginning and end of fatigue life. In addition, many events occur at the low load portion of the fatigue cycle. Internal rubbing surfaces were proposed as a source for these events. The authors suggest that LMCs at the stress concentration notches create these surfaces and are currently working on correlations between mechanical hysterisis and acoustic events to verify this theory. Penetrant enhanced X-ray radiography, ultrasonic C-scan and optical microscopy were also demonstrated to be useful for locating and characterizing compressive fatigue damage in thick composite laminates.

ACKNOWLEDGMENTS

This research is funded by the Defense Advanced Research Projects Agency, program manager Mr. James J. Kelly, through the Office of Naval Research, Mechanics Division, Dr. Yapa D.S. Rajapakse, DARPA agent. The authors would also like to thank the many faculty and students at The Johns Hopkins University who have made numerous contributions to this research.

REFERENCES

1. G.M. Wood, Proc. Fourth Annual Thick Composites in Compression Workshop, iii, 1990.
2. K.L. Reifsnider, Fatigue of Composite Materials, edited by K.L. Reifsnider, (Elsevier Science Publishers B.V., 1990).
3. R. Talreja, Fatigue of Composite Materials, edited by R. Talreja, (Technomic Publishing Co., Inc., 1987).
4. W.W. Stinchcomb and C.E. Bakis, Fatigue of Composite Materials, edited by K.L. Reifsnider, (Elsevier Science Publishers B.V., 1990), p. 163.
5. W. Hwang, Composite Materials: Fatigue and Fracture, Second Volume, ASTP STP 1012, Paul A. Lagace, Ed., American Society For Testing Materials, Philadelphia, 1987, pp. 87-102.
6. H.T. Hahn and J.G. Williams, Composite Materials: Testing and Design (seventh conference), ASTM STP 893, J.M. Whitney, Ed., American Society For Testing Materials, Philadelphia, 1986, pp. 115-139.
7. P.A. Lagace and S.C. Nolet, Composite Materials: Fatigue and Fracture, ASTM STP 907, H.T. Hahn, Ed., American Society For Testing Materials, Philadelphia, 1986, pp.335-360.